DOE-ER63616-FINAL REPORT

Interfacial Reduction-Oxidation Mechanisms Governing Fate and Transport of Contaminants in the Vadose Zone

Principal Investigator: Baolin Deng
University of Missouri, Columbia, MO
DengB@missouri.edu

Co-Principal Investigator: Silvia Sabine Jurisson
University of Missouri, Columbia, MO

Co-Principal Investigator: Edward C. Thornton
Pacific Northwest National Laboratory
Richland, WA

Co-Principal Investigator: Jeff Terry
Illinois Institute of Technology, Chicago, IL

U.S. Department of Energy
Grant Number: DE-FG02-03ER63616
Grant Project Officer: Roland Hirsch
Project Duration: (October 2003 – December 2007)

ACKNOWLEDGMENTS

This project is supported by the Environmental Remediation Science Program (ERSP) of the Office of Science and Technology of the U.S. Department of Energy. The research was conducted at the University of Missouri (MU), the Pacific Northwest National Laboratory (PNNL), and Illinois Institute of Technology. Contributions of all research scientists, postdoctoral associates, and students to this project are greatly appreciated. These individuals, as indicated by coauthors of various papers, include Bin Hua, Yongjian Liu (MU), Chulsung Kim (Georgia Gwinnett College), Yeqing Lan (Nanjing Agricultural University), Youxian Wu (San Diego State University), Mart Oostrom, Lirong Zhong, James E. Amonette (PNNL), John Yang (Lincoln University of Missouri), Huifang Xu, and Hiromi Kornishi (University of Wisconsin-Madison).

I. Research Objectives:

There are many soil contamination sites at the Department of Energy (DOE) installations that contain radionuclides and toxic metals such as uranium (U), technetium (Tc), and chromium (Cr). Since these contaminants are the main "risk drivers" at the Hanford site (WA) and some of them also pose significant risk at other DOE facilities (e.g., Oak Ridge Reservation - TN; Rocky Flats - CO), development of technologies for cost effective site remediation is needed. Current assessment indicates that complete removal of these contaminants for *ex-situ* disposal is infeasible, thus *in-situ* stabilization through reduction to insoluble species is considered one of the most important approaches for site remediation. *In Situ* Gaseous Reduction (ISGR) is a technology developed by Pacific Northwest National Laboratory (PNNL) for vadose zone soil remediation. The ISGR approach uses hydrogen sulfide (H_2S) for reductive immobilization of contaminants that show substantially lower mobility in their reduced forms (e.g., Tc, U, and Cr). The technology can be applied in two ways: (i) to immobilize or stabilize pre-existing contaminants in the vadose zone soils by direct H_2S treatment, or (ii) to create a permeable reactive barrier (PRB) that prevents the migration of contaminants. Direct treatment involves reduction of the contaminants by H_2S to less mobile species. Formation of a PRB is accomplished through reduction of ferric iron species in the vadose zone soils by H_2S to iron sulfides (e.g., FeS), which provides a means for capturing the contaminants entering the treated zone. Potential future releases may occur during tank closure activities. Thus, the placement of a permeable reactive barrier by ISGR treatment can be part of the leak mitigation program. Deployment of these ISGR approaches, however, requires a better understanding of the immobilization kinetics and mechanisms, and a better assessment of the long-term effectiveness of treatment.

The primary objective of this project was to understand the complex interactions among the contaminants (i.e., Cr, Tc, and U), H_2S, and various soil constituents. The reaction with iron sulfide is also the focus of the research, which could be formed from iron oxide reduction by hydrogen sulfide. Factors controlling the reductive immobilization of these contaminants were identified and quantified. The results and fundamental knowledge obtained from this project shall help better evaluate the potential of *in situ* gaseous treatment to immobilize toxic and radioactive metals examined.

II. Project Results and Information Access

Collaborative researches under this project, including the University of Missouri, Pacific Northwest National Laboratory, and Illinois Institute of Technology, have greatly improved our understanding of the interactions among H_2S, the metal contaminants, and soil components. Detailed kinetics and mechanism have been established for reactions of Cr(VI), U(VI), and Tc(VII) with sulfides. Some design related issues for effective application of the ISTR technology have also been addressed.

Under this project, seventeen (17) journal articles and one (1) report have been published as listed below. Since these journal papers are easily accessible as open literatures, here we provide only abstracts of the papers in the report, except one manuscript under review (Reductive precipitation of uranium(VI) by amorphous iron sulfide), for which the full paper is provided in Appendix A.

1. Hua, B.; Deng, B. (2008) "Reductive precipitation of uranium(VI) by amorphous iron sulfide". ***Environ. Sci. Technol***. (In review. Included as part of this report).

2. Zhong, L.; Thornton, E. C.; Deng, B. (2007) "Uranium immobilization by hydrogen sulfide gaseous treatment under vadose zone conditions". ***Vadose Zone Journal***, *6*, 149-157.

3. Thornton, E. C.; Zhong, L.; Oostrom, M.; Deng, B. (2007) "Experimental and theoretical assessment of the lifetime of a gaseous-reduced vadose zone permeable reactive barrier". ***Vadose Zone Journal***, *6*, 1050-1056.

4. Liu, Y.; Terry, J.; Jurisson, S. (2007) "Pertechnetate immobilization in aqueous media with hydrogen sulfide under anaerobic and aerobic environments". ***Radiochimica Acta***, *95*, 717-725.

5. Liu, Y., J. Terry, and S. Jurisson (2007) "Pertechnetate immobilization with amorphous iron sulfide", ***Radiochimica Acta*** (submitted).

6. Hua, B.; Yang, J.; Deng, B. (2007) "Radioactive Wastes", ***Water Environ. Research****,* (Literature Review), *79*, 1903-1928.

7. Hua, B.; Deng, B.; Thornton, E. C.; Yang, J.; Amonette, J. E. (2007) "Incorporation of chromate into calcium carbonate structure during coprecipitation". ***Water, Air, and Soil Pollution***, *179*, 381-390.

8. Lan, Y.; Deng, B.; Kim, C.; Thornton, E. C. (2007) "Influence of soil minerals on chromium(VI) reduction by sulfide under anoxic conditions". ***Geochemical Transactions***, *8:4,* 1-10.

9. Kim, C.; Lan, Y.; Deng, B. (2007) "Kinetic study of hexavalent Cr(VI) reduction by hydrogen sulfide through geothite surface catalytic reaction". ***Geochemical Journal***, *41*, 397-405.

10. Lan, Y.; Yang, J.; Deng, B. (2006) "Catalysis of dissolved and adsorbed iron in soil suspension on chromium(VI) reduction by sulfide", ***Pedosphere****, 16(5)*: 572-578.

11. Hua, B.; and Deng, B. (2006) "Radioactive Wastes", ***Water Environ. Research,*** (Literature Review), *78*, 1856-1882.

12. Wu, Y. and Deng, B. (2006) "Effects of FeS on chromium oxidation mediated by manganese oxidizers", ***Environmental Engineering Science***, *23(3)*: 552-560.

13. Thornton, E. C.; Zhong, L.; Oostrom, M. (**2006**) "Development of a field design for in situ gaseous treatment of sediment based on laboratory column test data". ***Journal of Environmental Engineering***, *132*, 1626-1632

14. Hua, B.; Xu, H.; Terry, J.; Deng, B. (2006) "Kinetics of uranium(VI) reduction by hydrogen sulfide in anoxic aqueous systems". ***Environ. Sci. Technol***., *40*, 4666-4671.

15. Zhong, L., and E.C. Thornton (2006) "Laboratory Evaluation of Uranium Immobilization in the Vadose Zone by Hydrogen Sulfide Gaseous Reduction of Hanford Formation Sediment", Section 3.3.8 in *Hanford Site Groundwater Monitoring for Fiscal Year 2005*, M.J. Hartman, L.F. Morasch, and W.D. Webber (eds.), Pacific Northwest National Laboratory, PNNL-15670.

16. Hua, B.; and Deng, B. (2005) "Radioactive Wastes", ***Water Environ. Research,*** (Literature Review), *77*, 2244-2298.

17. Wu, Y., Deng, B. and Xu, H.; Kornishi, H. (2005) "Chromium(III) Oxidation Coupled with Microbially-Mediated Mn(II) Oxidation", ***Geomicrobiology Journal***, *22*, 161-170.

18. Lan, Y., Deng, B.; Kim, C., Thornton, E., and Xu, H. (2005) "Catalysis of Elemental Sulfur Nanopartiles on Cr(VI) Reduction by Hydrogen Sulfide", ***Environ. Sci. Technol***. *39*, 2087-2094.

III. Abstracts

A - Research on uranium

A-1. Kinetics of uranium(VI) reduction by hydrogen sulfide in anoxic aqueous systems.

Hua, B.; Xu, H.; Terry, J.; Deng, B

(*Environmental Science and Technology* **2006**, *40*, 4666-4671.)

Uranium (U) is the single most frequently detected radionuclide contaminant in groundwater and soils at DOE facilities. It is redox-sensitive under ambient environments and its mobility depends greatly on its redox speciation: U(VI) species (e.g., $UO_2(OH)^+$, $UO_2(CO_3)_3^{4-}$) are much more mobile than U(IV) species (e.g., $UO_{2(s)}$). Elucidating the factors that control uranium redox transformation rates is critical to many important processes such as: (i) formation of U mineral deposits, (ii) selection of radioactive waste repositories; and (iii) remediation of U-containing waste sites. In this study, we investigated the kinetics of U(VI) reduction by hydrogen sulfide in anaerobic aqueous systems, in which the pH was varied from 6.37 to 9.06 and carbonate concentration from 0.0 to 30.0 mM. The results obtained at pH 6.89 and 4.0 mM of $[CO_3^{2-}]_{total}$ showed that the ratio of U(VI) reduced to sulfide consumed was 0.94. This observation suggested that the reaction stoichiometry was:

$$UO_2^{2-} + S^{2-} = UO_2 + S$$

At the same pH $[CO_3^{2-}]_{total}$ conditions, the reaction kinetics were observed to be:

$$-\frac{d[U(VI)]}{dt} = 0.0084[U(VI)][H_2S]_{Total}^{0.82}$$

We found that the rate of U(VI) reduction was largely controlled by the solution pH and carbonate concentration. As shown by Figure 1, the reduction was almost completely inhibited with the following $[CO_3^{2-}]_{total}$ and pH combinations: [(≥15.0 mM, pH 6.89); (≥4.0 mM, pH 8.01); and (≥4.0 mM, pH 9.06)]. Extensive modeling study was conducted to determine the relationship between speciation and reactivity. By comparing the calculated carbonate - U(VI) and hydroxo - U(VI) speciation with the measured reaction rates Figure 2, we found that carbonate-U(VI) complexes were not the major species reduced, instead, we believe that hydroxo-U(VI) complexes were reduced under the experimental conditions.

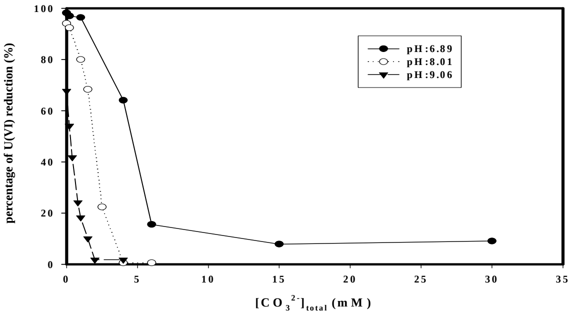

Figure 1. Effects of $[CO_3^{2-}]$total on U(VI) reduction at fixed pH of 6.89, 8.01, or 9.06

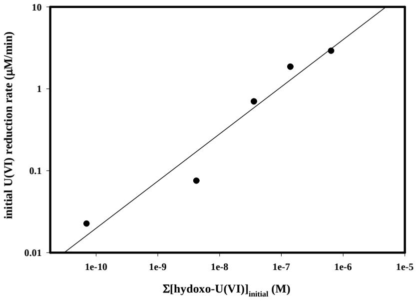

Figure 2. Initial rate of U(VI) reduction as a function of total [hydroxo –U(VI)] species in systems with various $[CO_3^{2-}]$ concentrations

A-2. Reductive precipitation of uranium(VI) by amorphous iron sulfide

Hua, B.; Deng, B.

(*Environmental Science and Technology, **2008***. In review. Full manuscript is included as Appendix A)

Batch experiments were used to evaluate the reductive immobilization of hexavalent uranium (U(VI)) by synthesized, amorphous iron sulfide (FeS) in the anoxic environment. The tests were initiated by spiking 168.0 μM U(VI) to 0.18 g/L FeS suspensions at pH varied from 5.99 to 10.17. The uptake of U(VI) was determined by monitoring the changes in aqueous U(VI) concentration, and the reduction of sorbed U(VI) was determined by the difference between the total spiked U(VI) and the extractable amount of U(VI) by 25 mM $NaHCO_3$ solution. The results showed that a rapid uptake of U(VI) by FeS occurred within one hour under all pH conditions accompanied by simultaneous release of Fe(II); whereas the reduction of sorbed U(VI) took hours to over a week for completion. The reduction followed a pseudo-first-order kinetics and the rate was strongly dependent on the solution pH. Product analysis by X-ray photoelectron spectroscopy showed the formation of U_3O_8/UO_2 and polysulfide, but no ferric iron was detected. This suggested that U(VI) reduction was by reduced sulfur species, instead of Fe(II) species.

A-3. Uranium immobilization by hydrogen sulfide gaseous treatment under vadose zone conditions.

Zhong, L.; Thornton, E. C.; Deng, B.
(*Vadose Zone Journal* **2007**, *6*, 149-157)

Mobility of hexavalent uranium [U(VI)] in H_2S-treated soils was investigated using laboratory column experiments to assess the potential of applying in situ gaseous reduction for U immobilization in the vadose zone. Soil from the Hanford Formation in the U.S. Department of Energy Hanford Site, Washington, was used in this study. The impact of water chemistry and soil treatment on U(VI) immobilization and the role of gas humidity on soil treatment were investigated. The study revealed that soil uptake of U(VI) from deionized water was much higher than that from the simulated Hanford groundwater. Nevertheless, gas-treated soil was still shown to have the potential for immobilizing U(VI) from the simulated groundwater. In addition, changes in H_2S column breakthrough indicated that humidity enhanced the reduction of soil Fe. In the first 20 pore volumes, the soil treated with moisturized H_2S gas can effectively immobilize >80% of the mobile U(VI). Primary mechanisms for U immobilization included U(VI) sorption to the sediments, reduction of U(VI) to insoluble U(IV), and enhanced adsorption of U(VI) to newly formed Fe oxides. Remobilization of U following reoxidation of the sediment was relatively insignificant under the experimental conditions applied, apparently owing to the enhanced adsorption of U to poorly crystallized hydrous ferric oxide products.

A-4. Experimental and theoretical assessment of the lifetime of a gaseous-reduced vadose zone permeable reactive barrier.

Thornton, E. C.; Zhong, L.; Oostrom, M.; Deng, B.
(*Vadose Zone Journal* **2007**, *6*, 1050-1056)

The feasibility of using in situ gaseous reduction to establish a vadose zone permeable reactive barrier was evaluated through a combination of laboratory testing and consideration of fundamental vadose zone transport concepts. For the experimental evaluation, a series of laboratory column tests were conducted in which Hanford formation sediment from the USDOE Hanford Site in Richland, WA, was first treated with a diluted hydrogen sulfide gas mixture to reduce sediment iron oxide to ferrous sulfide. Water containing dissolved oxygen was then pumped through the columns at different flow rates to determine the reoxidation rate and the reductive capacity of the treated sediment. The results indicated that the treated sediment has a significant reductive capacity consistent with the basic reactions associated with the treatment and reoxidation processes. The observed reductive capacity was found to be dependent on the flow rate of water during the reoxidation phase of the tests. The reductive capacity approached the maximum value predicted on the basis of the treatment reaction as the flow rate was decreased. Thus, laboratory treatment tests provide a means for predicting the reductive capacity of the barrier under field conditions. In the theoretical assessment, oxygen diffusion was identified as the dominant mechanism leading to reoxidation of the barrier. Depending on vadose zone characterisitics, the predicted barrier lifetime varies from several years to more than 100 years.

A-5. Development of a field design for in situ gaseous treatment of sediment based on laboratory column test data.

Thornton, E. C.; Zhong, L.; Oostrom, M.
(*Journal of Environmental Engineering* **2006**, *132*, 1626-1632)

A testing methodology is presented that supports the development of a field design for in situ gaseous treatment of sediments with diluted hydrogen sulfide. This approach involves the collection of column breakthrough test results at various flow rates, allowing a relationship to be developed between pore velocity of the carrier gas and velocity of the hydrogen sulfide reaction front that permits sizing to the field scale. A regression fit of a set of laboratory column breakthrough test data collected in this study is utilized to illustrate the development of a field design based on a two-dimensional radial flow analytical model. Information regarding treatment time and hydrogen sulfide consumption characteristics associated with in situ gaseous treatment can then be obtained from this model and used as a basis for estimation of treatment schedule and costs. The regression relationship can also be utilized in numerical models in more complex geometries to support the field design of in situ gaseous treatment operations.

B - Research on technetium

B-1. Pertechnetate immobilization in aqueous media with hydrogen sulfide under anaerobic and aerobic environments.

Liu, Y.; Terry, J.; Jurisson, S.
Radiochimica Acta **2007**, *95*, 717-725.

The basic chemistry for the immobilization of pertechnetate (TcO_4^-) by hydrogen sulfide was investigated in aqueous solution under both aerobic and anaerobic environments. Pertechnetate immobilization was acid dependent, with accelerated rates and increased immobilization yields as the acid concentration increased. Oxygen had no effect under acidic conditions. Under anaerobic alkaline conditions, the pH, and therefore the speciation of sulfide, was the determining factor on the immobilization of pertechnetate. Only 53% of the $TcO_4^-$was immobilized at pH 8, while the yield increased to 83% at pH 9 as HS^- became the dominant sulfide species. The immobilization yield then decreased to 73% at pH 13. No reaction was observed between TcO_4^- and sulfide under aerobic alkaline conditions, indicating that oxygen suppressed this reaction. Pertechnetate immobilization was found to be first order with respect to both sulfide and pertechnetate in acidic solutions, and in alkaline solution under anaerobic conditions. The results of stoichiometry studies and product analysis under alkaline anaerobic environments indicated that Tc_2S_7 was obtained at pH 9. EXAFS (extended X-ray absorption fine structure) and XANES (X-ray absorption near edge structure) studies suggested that the samples obtained from acidic, aerobic solution and alkaline anaerobic solution were both Tc_2S_7. The stability of Tc_2S_7 is affected by O_2 with accelerated dissolution at high pH.

B-2. Pertechnetate immobilization with amorphous iron sulfide.

Liu, Y., J. Terry, and S. Jurisson
(Radiochimica Acta, submitted.).

The studies reported on the reductive immobilization of TcO_4^- in aqueous solution with synthetic amorphous FeS_{am} under anaerobic environments showed a high reductive capacity of 867 mg Tc (VII)/g FeS_{am}. The reaction between FeS_{am} and TcO_4^- was pH dependent and was accelerated with increasing ionic strength. The reaction was assumed to be a surface mediated reaction through a ligand exchange mechanism to generate an outer-sphere complex according to the models. The characterization of the product generated from the TcO_4^- -FeS_{am} reaction showed it to be TcO_2, which showed remarkable stability under anaerobic environments, suggesting the potential for in situ immobilization of TcO_4^- in the vadose zone by H_2S gas when iron-containing minerals are present. A reaction stoichiometry was hypothesized based on the solution analysis and sample characterization.

C - Research on chromium

C-1. Incorporation of chromate into calcium carbonate structure during coprecipitation.

Hua, B.; Deng, B.; Thornton, E. C.; Yang, J.; Amonette, J. E.
(*Water, Air, and Soil Pollution* **2007**, *179*, 381-390).

To assess treatment technologies and establish regulatory framework for chromate-contaminated site remediation, it is imperative to know the exact chromium speciation in soil matrices. In a previous study on chromium speciation in soil by sequential solution extraction, we found that there was a fraction of non-extractable chromate present in soil samples from Hanford Site, Washington and it was hypothesized that this non-extractable chromate resided in the structure of minerals such as calcite. To test this hypothesis, a number of calcite precipitates were prepared in the presence of various concentrations of chromate during the precipitation, which could coprecipitate chromate, or by adding chromate after the precipitation was completed. Hydrochloric acid was used to dissolve calcite and therefore extract the coprecipitated and surface attached chromate. The results showed that the coprecipitated chromate was non-extractable by hot alkaline solution or phosphate buffer, but could be solubilized by HCl in proportional to the amount of calcite dissolved. The X-ray diffraction experiments revealed that the coprecipitation of chromate with calcite had an influence on its crystal structure: the higher the chromate concentration, the greater the ratio of vaterite to pure synthetic calcite

C-2. Catalysis of elemental sulfur nanoparticles on chromium(VI) reduction by sulfide under anaerobic conditions.

Lan, Y.; Deng, B.; Kim, C.; Thornton, E. C.; Xu, H.
(*Environmental Science and Technology* **2005**, *39*, 2087-2094).

Chromate (Cr^{VI}) reduction by sulfide was conducted in anaerobic batch experimental systems. The molar ratio of the reduced Cr^{VI} to the oxidized S^{II-} was 1:1.5 during the reaction, suggesting that the product of sulfide oxidation was elemental sulfur. Under the anaerobic condition, the reaction was pseudo first order initially with respect to Cr^{VI}, but the rate was dramatically accelerated at the later stage of the reaction. The rate acceleration was due to catalysis by elemental sulfur nanoparticles; dissolved species such as monomeric elemental sulfur and polysulfides appeared to be ineffective catalysts. Elemental sulfur nanoparticles were capable of adsorbing sulfide and such adsorbed sulfide exhibited much higher reactivity towards Cr^{VI} reduction than the aqueous phase sulfide, resulting in the observed rate acceleration. Kinetic data under various reactant concentrations can be represented by the following empirical kinetic equation:

$$-\frac{d[Cr^{VI}]}{dt} = k_1 [Cr^{VI}][H_2S]^{0.63} + k_3 [Cr^{VI}] [\equiv\text{S-SH}]^{0.57}$$

The first term on the r.h.s. corresponds to the non-catalytic pathway, with $k_1 = 1.0\text{x}10^{-3}$ $(\mu M)^{-0.63}$ min^{-1} at pH 7.60 and $8.2\text{x}10^{-5}$ $(\mu M)^{-0.63}$ min^{-1} at pH 8.10. The second term, k_3 $[Cr^{VI}]$ $[\equiv\text{S-SH}]^b$, is the catalytic term with [≡S-SH] representing the adsorbed concentration of sulfide on the elemental sulfur nanoparticles (μM). The catalytic term is more important at the later stage of the reaction, as indicated by the observed kinetics and the enhancement of the reaction rate by externally-added elemental sulfur nanoparticles. At pH 8.10, $k_3 = 0.0057$ $(\mu M)^{-0.57}$ min^{-1}.

C-3. Influence of soil minerals on chromium(VI) reduction by sulfide under anoxic conditions.

Lan, Y.; Deng, B.; Kim, C.; Thornton, E. C.
(*Geochemical Transactions* **2007**, *8:4,* 1-10).

The effects of soil minerals on chromate ($Cr^{VI}O_4^{2-}$, noted as Cr(VI)) reduction by sulfide were investigated in the pH range of 7.67 to 9.07 under the anoxic condition. The examined minerals included montmorillonite (Swy-2), illite (IMt-2), kaolinite (KGa-2), aluminum oxide (γ-Al_2O_3), titanium oxide (TiO_2, P-25, primarily anatase), and silica (SiO_2). Based on their effects on Cr(VI) reduction, these minerals were categorized into three groups: (i) minerals catalyzing Cr(VI) reduction – illite; (ii) minerals with no effect – Al_2O_3; and (iii) minerals inhibiting Cr(VI) reduction- kaolinite, montmorillonite, SiO_2 and TiO_2 . The catalysis of illite was attributed primarily to the low concentration of iron solubilized from the mineral, which could accelerate Cr(VI) reduction by shuttling electrons from sulfide to Cr(VI). Additionally, elemental sulfur produced as the primary product of sulfide oxidation could further catalyze Cr(VI) reduction in the heterogeneous system. Previous studies have shown that adsorption of sulfide onto elemental sulfur nanoparticles could greatly increase sulfide reactivity towards Cr(VI) reduction. Consequently, the observed rate constant, k_{obs}, increased with increasing amounts of both iron solubilized from illite and elemental sulfur produced during the reaction. The catalysis of iron, however, was found to be blocked by phenanthroline, a strong complexing agent for ferrous iron. In this case, the overall reaction rate at the initial stage of reaction was pseudo first order with respect to Cr(VI), i.e., the reaction kinetics was similar to that in the homogeneous system, because elemental sulfur exerted no effect at the initial stage prior to accumulation of elemental sulfur nanoparticles. In the suspension of kaolinite, which belonged to group (iii), an inhibitive effect to Cr(VI) reduction was observed and subsequently examined in more details. The inhibition was due to the sorption of elemental sulfur onto kaolinite, which reduced or completely eliminated the catalytic effect of elemental sulfur, depending on kaolinite concentration. This was consistent with the observation that the catalysis of externally added elemental sulfur (50 μM) on Cr(VI) reduction would disappear with a kaolinite concentration of more than 5.0 g/L. In kaolinite suspension, the overall reaction rate law was:

$$-d[Cr(VI)]/dt = k_{obs}[H^+]^2[Cr(VI)][HS^-]^{0.70}$$

C-4. Kinetic study of hexavalent Cr(VI) reduction by hydrogen sulfide through goethite surface catalytic reaction.

Kim, C.; Lan, Y.; Deng, B.
Geochemical Journal **2007**, *41*, 397-405.

Among metal oxides and clay minerals, goethite was in unique in terms of its effect on Cr(VI) reduction by hydrogen sulfide, because reductive dissolution of iron oxide by sulfide occurred, so Cr(VI) reduction was influenced by both dissolved ferrous iron and iron oxide surfaces. The effect was examined primarily at pH 8.45 (controlled by borate buffer) and an ionic strength of 0.20 M (controlled by $NaClO_4$). Preliminary tests showed that when solution pH was less than 8.4, the reduction rate of Cr(VI) by H_2S in the presence of goethite was too fast for data collection using our specific experimental setup. All tests were conducted under anaerobic conditions. Experimental data showed that the reduction rate was strongly dependent upon the initial concentrations of goethite (Figure3-a), Cr(VI) (Figure3-b), and sulfide (Figure3-c). In the presence of 0.33 g/L of goethite, the observed kinetic constant was about 5 times higher than that without goethite. The rate enhancement resulted from both surface catalysis and ferrous iron produced, which served as a catalyst.

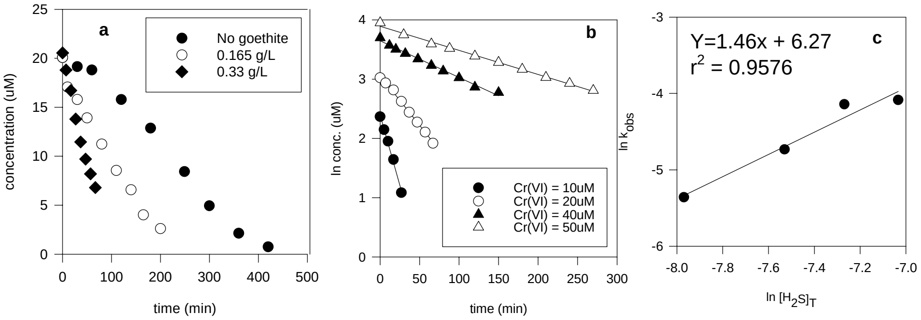

Figure 3. Effect of goethite in Cr(VI) reduction by sulfide under various concentrations of goethite (a), Cr(VI) (b), and sulfide (c).

When more surface area was provided, the reduction rate increased, suggesting that surface site availability for either Cr(VI) and/or sulfide was an important factor controlling the reduction rate. The limitation of surface sites was also consistent with the results at various initial Cr(VI): the rate constant at lower initial Cr(VI) was higher, probably due to the relatively larger portion of Cr(VI) adsorption onto the goethite surface, in comparison with the systems with higher initial Cr(VI). For aqueous Cr(VI) reduction by hydrogen sulfide, we had demonstrated that the reaction was first order with respect to both sulfide and Cr(VI). Experiments in the system with goethite, however, showed a reaction order of 1.5 in sulfide (Fig.3-c), suggesting a change of reaction mechanisms.

C-5. ***Chromium(III) oxidation coupled with microbially-mediated Mn(II) oxidation***

Wu, Y., Deng, B. and Xu, H., Kornishi, H.
(*Geomicrobiology Journal*, **2005**, 22, 161-170).

Reductive immobilization of Cr(VI) has been widely explored as a cost-effective approach for Cr-contaminated site remediation. In soils containing manganese, however, the immobilized form of chromium, i.e., Cr(III), could potentially be re-oxidized. In this study, batch experiments were conducted to assess whether there were any microbial processes that could accelerate Cr(III) oxidation in aerobic, manganese-containing systems. The results showed that in the presence of at least one species of manganese oxidizers, *Pseudomonas putida*, Cr(III) oxidation took place at low concentrations of Cr(III). About 30-50% of added Cr(III) (10 – 200 μM) was oxidized to Cr(VI) within five days in the systems with *P. putida* and biogenic Mn oxides. The rate of Cr(III) oxidation was approximately proportional to the initial concentration of Cr(III) up to 100 μM, but the growth of *P. putida* was partially inhibited by Cr(III) at 200 μM and totally stopped when it reached 500 μM. Cr(III) oxidation was dependent upon the biogenic formation of Mn oxides, though the oxidation rate was not directly proportional to the amount of Mn oxides formed. Chromium(III) oxidation took place through a catalytic pathway, in which the microbes mediated Mn(II) oxidation to form Mn-oxides, and Cr(III) was subsequently oxidized by the biogenic Mn-oxides.

C-6. ***Inhibition of FeS on chromium(III) oxidation by biogenic manganese oxides***

Wu, Y., Deng, B.
(*Environmental Engineering Science*, **2006**, *23(3)*: 552-560).

Reductive immobilization of Cr(VI) has been widely explored as a cost-effective approach for soil and water remediation. The long-term stability of the immobilized Cr(III), however, has to be addressed for the immobilization technology to be widely deployed. Cr(III) can be oxidized chemically by Mn-oxides produced through microbially-mediated Mn(II) oxidation. Whether Cr(III) could be remobilized through the oxidation process under more specific environmental conditions, however, needs to be investigated. This study examined the inhibitive effect of FeS on Cr(III) oxidation by biogenic Mn-oxides that were produced in the culture of a known species of Mn(II) oxidizers, Pseudomonas putida. The results showed that 120 mg/l of well-aged Merck granular FeS did not affect Cr(III) oxidation in the culture of *P. putida* initially containing Mn(II). In contrast, freshly precipitated FeS slurry at a much lower concentration (10 mg/l) significantly delayed Mn-oxide production and Cr(III) oxidation, without affecting the microbial growth. In the presence of excessive FeS slurry, both Cr(VI) and biogenic Mn oxides were reduced rapidly. The reduced Cr(III) was not re-oxidized by biogenic Mn-oxides as long as freshly formed FeS was present in the systems. The study suggested that FeS produced during the soil and water treatment by technologies such as *In-Situ* Gas Reduction (ISGR) could inhibit Mn(II) oxidation and thus prevent Cr(III) from reoxidation by biogenic Mn oxides.

C-7. Evaluation of the potential for long-term chromium re-oxidation in a H_2S-treated sediment sample

Thornton, C., Zhong, L., Deng, B.
(Unpublished data)

Hexavalent chromium in soil is readily reduced to the trivalent oxidation state by reaction with hydrogen sulfide. It is generally regarded as stable in this form in the natural environment and relatively insoluble. A long-term test has been conducted to provide information regarding whether or not reoxidation of chromium can occur after Cr(VI) is reduced in a contaminated sediment by hydrogen sulfide gas treatment.

In this test, a chromate-contaminated sediment sample collected from the 100K Area at the Hanford Site was treated with diluted hydrogen sulfide gas and then exposed to air under humid conditions. Analysis of the Cr(VI) content of the untreated and treated sediment was conducted by water leaching for one hour and measurement of Cr(VI) in the leachate by the diphenylcarbazide spectrophotometric method. The untreated sample contains about 110 mg/kg Cr(VI), while the treated sediment was determined to contain 3.3 mg/kg Cr(VI) initially. The results of the gas treatment test indicates that immobilization of Cr(VI) to Cr(III) is essentially quantitative although a portion of the chromate may be contained in solid waste phases.

The treated sample was exposed to air under humid conditions and sampled periodically and analyzed to determine if the concentration of Cr(VI) changes with time. Results obtained over a period of 2367 days of testing are shown in Figure 4. Levels of hexavalent chromium in the sediment dropped from about 3.3 mg/kg in the first year to a level ranging from 1.9 to 2.6 mg/kg. Samples collected at 492 days and later all contained about 2 mg/kg. The data suggests that a near steady state concentration had been attained in the long-range test, although a possible slowly declining trend can be seen. Data obtained from this test, which exceeds six years in duration, strongly suggests that reduced chromium will not reoxidize to the hexavalent state.

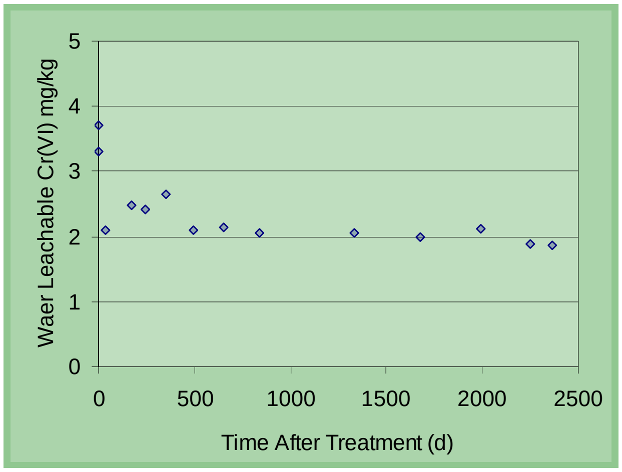

Figure 4. Water Leachable Cr(VI) Concentration vs. Time from a Contaminated Hanford Soil Treated with Hydrogen Sulfide

Appendix A

Reductive Precipitation of Uranium(VI) by Amorphous Iron Sulfide

Bin Hua and Baolin Deng

Environ. Sci. Technol. (manuscript in review).

Abstract

Batch experiments were used to evaluate the reductive immobilization of hexavalent uranium (U(VI)) by synthesized, amorphous iron sulfide (FeS) in the anoxic environment. The tests were initiated by spiking 168.0 μM U(VI) to 0.18 g/L FeS suspensions at pH varied from 5.99 to 10.17. The uptake of U(VI) was determined by monitoring the changes in aqueous U(VI) concentration, and the reduction of sorbed U(VI) was determined by the difference between the total spiked U(VI) and the extractable amount of U(VI) by 25 mM $NaHCO_3$ solution. The results showed that a rapid uptake of U(VI) by FeS occurred within one hour under all pH conditions accompanied by simultaneous release of Fe(II); whereas the reduction of sorbed U(VI) took hours to over a week for completion. The reduction followed a pseudo-first-order kinetics and the rate was strongly dependent on the solution pH. Product analysis by X-ray photoelectron spectroscopy showed the formation of U_3O_8/UO_2 and polysulfide, but no ferric iron was detected. This suggested that U(VI) reduction was by reduced sulfur species, instead of Fe(II).

Introduction

Sorption and reduction of U(VI) by a variety of minerals have strong influence on its mobility in the subsurface environment, and the immobilization processes are often controlled by water chemistry, such as solution pH and inorganic/organic ligands (Langmuir, 1978; Hsi and Langmuir, 1985; Ho and Doern, 1985; Ho and Miller, 1986; Payne and Waite, 1991; Wersin et al., 1994; Moyes et al., 2000; Giammer and Hering, 2001). The effects of pH and ligands on the sorption of U(VI) by iron (hydr)oxides have been well documented. For instance, it was found that U(VI) sorption by hematite started at pH 4, jumped to completion at pH 5.5, and remained complete to pH 7.6 (Liger et al., 1999). Similar behavior was observed for U(VI) sorption by Fe(III) oxides in the presence of carbonate ions (Waite et al., 1994); however, desorption of U(VI) was observed at pH $\geq$ 7.5. Further, the desorption edge of U(VI) was noticed to move to lower pH values as CO_2 partial pressure increased in an open system (Villalobos et al., 2001). The sorption of U(VI) by goethite was influenced by phosphate in a different way: at low pH, the higher the phosphate concentration, the more U(VI) was adsorbed; whereas at high pH, the opposite was observed (Cheng et al., 2004). The presence of natural organic matter, like phosphate, enhanced the sorption of U(VI) by hematite at low pH, but slightly hindered the sorption under alkaline conditions (Lenhart and Honeyman, 1999).

In an anoxic environment, the reduction of U(VI) to U_3O_8/UO_2 may occur if certain reductants are present. It has been noticed that formations of at least some uranium ores are linked to the iron redox cycling (Posey-Dowty et al. 1987). Laboratory observations on the reduction of U(VI) by Fe(II) as well as sulfide species are not all consistent. It is generally agreed that $Fe(II)_{(aq)}$ ((aq) denotes species in the aqueous phase) can not reduce $U(VI)_{(aq)}$ (Liger et al., 1999). Some studies (Liger et al., 1999; O'Loughlin et al., 2003; Missana et al., 2003) reported that both sorbed Fe(II) by iron oxide and structural Fe(II) in minerals can reduce U(VI) to U(IV). However, other studies (Nevin et al., 2000; Istok et al., 2004) reported that Fe(III) oxides could oxidize U(IV) and generate sorbed Fe(II) species.

Unlike aqueous Fe(II), sulfide ions are found capable of reducing U(VI) (Kochenov et al., 1978; Duff, 1997; Beyenal et al., 2004; Hua et al., 2006) and the major factors influencing the kinetics of U(VI) reduction include solution pH and bicarbonate concentration (Hua et al., 2006). Several minerals containing reduced sulfur species have also been found to reduce U(VI), although the information is mostly qualitative in nature. For instance, reduction of U(VI) by galena and pyrite under anoxic conditions yielded a mixture of U(VI)/U(IV) species and polysulfides (Wersin et al., 1994). Partial reduction of U(VI) was also detected on mackinawite (Moyes et al., 2000).

Our previous study has focused on the aqueous phase U(VI) reduction by sulfide (Hua et al.,, 2006), showing that the reduction kinetics was strongly controlled by solution pH and carbonate concentration, and the reaction products were primarily nano-sized uraninite (UO_2) and elemental sulfur. The objective of this paper is to examine the interactions of U(VI) and a synthesized, amorphous iron sulfide (FeS) in a CO_2-free anoxic environment. Efforts were devoted to separate sorption and reduction of U(VI) by FeS and identify the reaction products and mechanisms.

Experimental Methods

All experiments were conducted under anoxic conditions in a glovebox (Coy Laboratory Products Inc.) with ~5% H_2 balanced with ~95% N_2. Solutions were prepared with deionized and distilled water (DDW, 18.2 MΩ·cm, Millipore Co.), pretreated following a reported procedure to minimize oxygen (Hua et al., 2006). Glassware was cleaned with 1N HCl and rinsed with DDW prior to use. U(VI) standard solution (997±2mg/L), sodium sulfide, 1,10-phenanthroline, and ferrous chloride were purchased from Fisher Scientific Co. All reagents were of ACS reagent grade and used without further purification.

FeS Preparation and Characterization. FeS stock suspension was prepared by reaction of 1.0 M $FeCl_2$ and 1.0 M Na_2S (Patterson et al., 1997). The synthesized FeS particles were washed multiple times with DDW until soluble ferrous iron concentration ($[Fe(II)]_{aq}$) was less than10 μM, and then stored in a polyethylene bottle. The FeS solid concentration was determined to be 1.80 g FeS/L by the following procedure: (1) pipette 1.00 mL suspension to a 40-mL glass vial, (2) dissolve FeS with several drops of 1.0 M HCl, (3) transfer the solution into a 1 L volumetric flask and dilute to the mark with DDW, and (4) determine $[Fe(II)]_{aq}$ by the phenanthroline spectrophotometric method

(APHA, 1989). The precision of delivering FeS suspension by pipette was assessed by six replicate tests, in which 1.00-mL FeS suspension was pipetted to each 40-mL glass vial and analyzed for $[Fe(II)]_{aq}$, showing a standard deviation of less than 6%.

A portion of the FeS suspension was freeze-dried (4.5-L Benchtop Freeze Dryer, Labconco Co.) in an air-tight container. The obtained FeS particles were stored in the anoxic glovebox prior to crystal structure and specific surface area analyses. To determine the crystal structure, approximately 0.5 g of FeS particles was placed in a sample holder (24.5-mm in diameter and 1-mm in depth) and analyzed on a MiniFlex automated, microprocessor-controlled X-ray powder diffractometer, with Cu-Ka X-ray source and semiconductor detector (operated at 15 mA and 30 kV). The sample was scanned from 20 to 40^o 2θ-degree range, with a stepping rate of 0.01^o and scan rate of 2.0^o/min. The result confirmed that the sample was amorphous iron sulfide (JCPDS, 1987). The specific surface area was measured on a PMI Automated Brunauer-Emmett-Teller (BET) Sorptometer (Porous Materials, Inc.) with N_2 adsorption at -196 ^oC, yielding a value of $31m^2/g$.

Experiments on U(VI) Uptake and Reduction. Each test began by mixing 1.00-mL FeS stock suspension (1.80 g FeS/L), 7.0-mL DDW, and 2.00-mL U(VI) solution, in a 25-mL brown vial, with the pH of the mixture controlled by pre-adjusting the pH of DDW. At the end of the reaction, the pH was checked again, showing that it never exceeded 0.40 pH unit from the preset values. Mixing was maintained by magnetic stirring (Variomag, Poly 15) and temperature was controlled at 22±1ºC. The reaction progress was monitored by analyzing $[U(VI)]_{aq}$ (Teixeira et al., 1999; Hua et al., 2006) and $[Fe(II)]_{aq}$ (APHA, 1989) as a function of time. At each time point, one of the parallel reaction vials was sacrificed to collect 3 mL supernatant by filtration through a 0.2 μm nylon filter (Fisher Scientific Co.). A 1.00-mL of the filtrate was used to determine $[U(VI)]_{aq}$, and another 1.00-mL of the filtrate was used to determine $[Fe(II)]_{aq}$. The difference between the amount of initially spiked U(VI) ($[U(VI)]_0$) and $[U(VI)]_{aq}$ was considered the uptake by FeS ($[U]_{uptake} = [U(VI)]_0 - [U(VI)]_{aq}$), the amount lost from the aqueous phase due to sorption of U(VI) by FeS and/or reduction to U(IV).

We devoted significant effort to differentiate U uptake due to the sorption of uranyl ion ($[U(VI)]_{(s)}$) and the uptake caused by U(VI) reduction by FeS. To begin with, 10.0 mL of $NaHCO_3$ (50 mM) was added to a reaction vial parallel to the one used for measuring $[U(VI)]_{aq}$, and then U(VI) in the extractant ($[U(VI)]_{ex}$) was measured after two hours of extraction. Our preliminary experiments showed that the extraction efficiency did not change after 30 min of extraction. We considered $[U(VI)]_{ex}$ represented the sum of $[U(VI)]_{aq}$ and $[U(VI)]_s$ (i.e., $[U(VI)]_{ex} = [U(VI)]_{aq} + [U(VI)]_s$). Several lines of evidence supported this argument. (1) U(VI) could form strong complexes with carbonate ions (Langmuir, 1978**;** Ho and Miller, 1986), leading to the complete desorption of U(VI) from ferrihydrite (Waite et al., 1994) and hematite (Liger et al., 1999) under alkaline conditions. (2) Our preliminary tests showed that no U(VI) uptake by FeS occurred in the presence of 25 mM $NaHCO_3$ during a testing period of 72 hrs. (3) While complete uptake of U(VI) by FeS always occurred less than one hour of reaction (refer to Fig. A1 (a)), over 91% of $[U(VI)]_0$ could still be extracted at pH 8.82 after one hr of reaction, and over 87% of $[U(VI)]_0$ extracted at pH 10.17 even after two hrs (as shown in Fig.A3(a)), suggesting that U(VI)(s) was extractable by the bicarbonate solution. (4) Carbonate does not dissolve UO_2 (e.g., uraninite) even at concentrated concentrations (Buck et al., 1996), which eliminates the possibility of reoxidation of reduced U under the anoxic conditions used for extraction.

As a result, if no $U(VI)_{(s)}$ were reduced, $[U(VI)]_{ex}$ would always equal to $[U(VI)]_0$ in the system. Our observation, however, showed that $[U(VI)]_{ex}$ decreased with the reaction time, implying the reduction of U(VI) to U(IV) and formation of products such as uraninite that was not extractable by the bicarbonate solution in the anoxic environment (Liger et al., 1999). Consequently, the difference between $[U(VI)]_0$ and $[U(VI)]_{ex}$ was considered the amount of reduced U.

Reoxidation of the reduced U on FeS was also investigated. Four reaction vials were prepared at pH 6.90 following the U reduction procedure described above. After 6 hr, two vials were sacrificed to measure $[U(VI)]_{ex}$, showing that U(VI) uptake and reduction was completed within the time period. The other two samples were taken out of the anoxic glovebox and exposed to the ambient air with 0.21 atm of oxygen partial pressure. The samples were mixed by a magnetic stirring bar to facilitate oxygen transfer. After a 24-hr exposure, $[U(VI)]_{aq}$ and $[U(VI)]_s$ in these samples were measured to determine whether the reduced U was reoxidized.

All experiments were duplicated. The average results were reported and the associated error bars in Fig. A1, A2, and A3 represented the variation of data from the averages.

X-ray Photoelectron Spectroscopy (XPS) analysis. XPS analysis was conducted on a KRATOS model AXIS 165 XPS Spectrometer with an argon sputtering KRATOS Minibeam ion source**.** The sample was prepared by mixing 50 mL of 1683 μM U(VI) with 50 mL of 18.0 g/L FeS at pH 6.90 in a 200-mL polyethylene bottle for 24 hr. After removing most of the supernatant, FeS was washed with pretreated DDW three times and freeze-dried in an air-tight container for over 24 hr. The sample was initially tapped on a sample supporting plate, which was then placed in a chamber and vacuumed to $\sim 10^{-9}$ Torr. XPS measurements were conducted with monochromatic aluminum at 1486.6eV, pass energies between 20 and 50 eV.

Results

U(VI) Uptake by FeS. As shown in Fig. A1(a), uptake of $U(VI)_{(aq)}$ by FeS was over 90% within 15 min at pH values from 5.99 to 8.82 and within 60 min at pH 10.17. After three hours, U(VI)(aq) was below the detection limit of 0.4 μM for all systems.

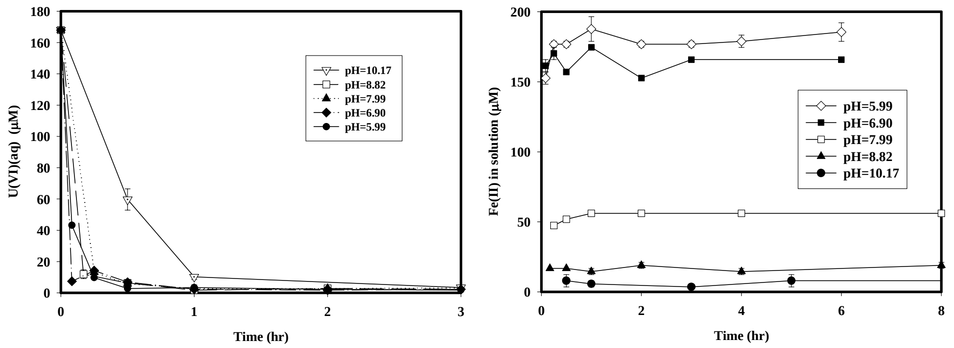

(a) **(b)**

FIGURE A1. Changes of $[U(VI)]_{aq}$ and $[Fe(II)]_{aq}$ with time. (a) U(VI) uptake was almost completed in one hour for all pHs; (b) solution pH has a strong impact on $[Fe(II)]_{aq}$. ($[U(VI)]_0$ = ~168.0 μM; [FeS] = 0.18 g/L).

The uptake of aqueous U(VI) by FeS particles was accompanied by the release of ferrous iron (Fe(II)) into the solution (Fig. A1(b)). Of particular interest was the final amount of soluble Fe(II) released (i.e, $[Fe(II)]_{aq}$) at pH 5.99 and 6.90, which was very close to the total amount of U(VI) associated with FeS (i.e., ~168 μM/L). At a higher pH value of 7.99, $[Fe(II)]_{aq}$ jumped from its background value of less than 10.0 μM to 47.0 μM within 15 min, increased to 56.0 μM in one hr, then remained nearly constant. Following this trend, $[Fe(II)]_{aq}$ was increased to approximately 18.0 μM at pH 8.82 within one hr and then remained constant, while there was no discernable increase in $[Fe(II)]_{aq}$ for over 8 hr at pH 10.17.

To establish the quantitative relationship between the uptake of U(VI) and release of Fe(II), we conducted an additional series of experiments at pH 6.90 with increasing $[U(VI)]_0$ from 42.0 to 420.0 μM. We found released $[Fe(II)]_{aq}$ was directly proportional to the total amount of U(VI) removed (R^2 = 0.997), with a $[U(VI)]_0/[Fe(II)]_{aq}$ ratio of 0.85±0.03 (within 90% confidence level) (Figure A2).

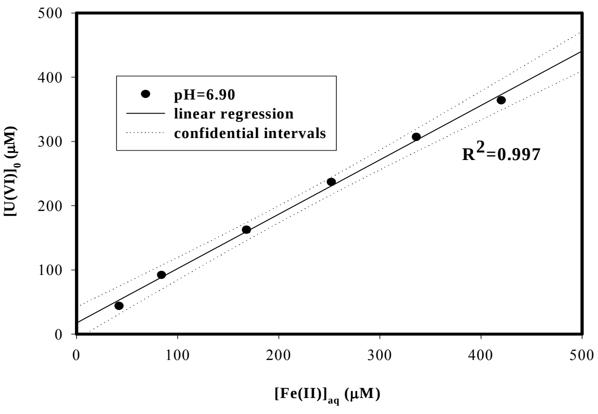

FIGURE A2. $[U(VI)]_0$ versus $[Fe(II)]_{aq}$ at pH 6.90. $[U(VI)]_0/[Fe(II)]_{aq}$ ratio is 0.85±0.03 (within 90% confidence level). The variation for the tests with $[U(VI)]_0$ = 168.3 μM is ±4.4%.

Reduction Rates of the U(VI) associated with FeS at Various pHs. The reduction of the U(VI) associated with FeS was monitored by measuring the concentration of extractable U(VI) ($[U(VI)]_{ex}$) as a function of time. As illustrated in Fig. A3(a), $[U(VI)]_{ex}$ decreased steadily with time, with the reduction rates strongly dependent on the solution pH. For instance, in the suspensions with pH 5.99 or 6.90, $[U(VI)]_{ex}$ was decreased to less than 50% of $[U(VI)]_0$ after 2 hrs and near nil after 4 hrs. At pH 7.99, $[U(VI)]_{ex}$ was decreased by approximately 50% after 4 hrs and to less than 10.0 μM after 18 hrs. In comparison, 50% of U(VI) reduction took approximately 20 hrs at pH 8.82 and 110 hrs at pH 10.17.

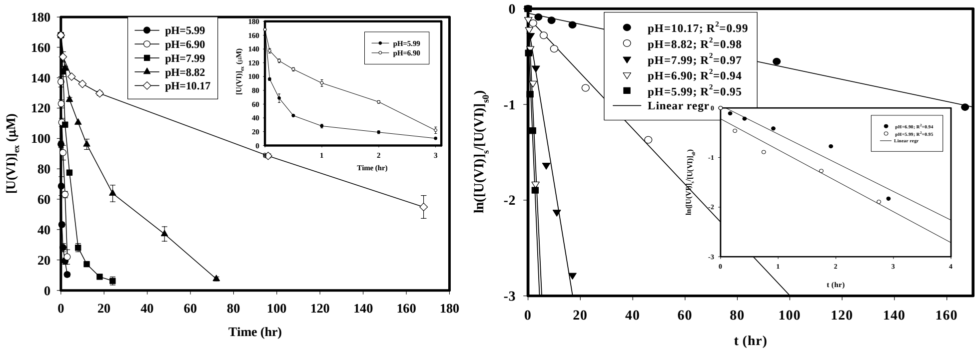

(a) (b)

FIGURE A3. (a) Changes of $[U(VI)]_{ex}$ with time at different pHs. The inset highlighted $[U(VI)]_{ex}$ changes at pH 5.99 and 6.90. The steady decreases in $[U(VI)]_{ex}$ are indicative of the reduction of $U(VI)_{(s)}$; (b) Plots of ln ($[U(VI)]_s/[U(VI)]_{s0}$) vs time at various pHs, suggesting the reaction follows a pseudo-first-order kinetic law.

Potential reoxidation and dissolution of reduced U was assessed by exposing the reduced samples at pH 6.99 to the ambient atmosphere for 6 hr under complete mixing conditions. The results showed that 62% of the reduced U was reoxidized, of which 11% was found in the aqueous phase and 89% associated with the solid phase.

Reaction Products. Chemical compositions of the solid products were analyzed by XPS , using pure FeS powder as a reference material when relevant. The XPS spectra of U4*f* for the reacted sample were shown in Fig. A4(a), with the blue line representing the outer surface scan and the red line the scan after argon etching to remove ~ 75 Å of the surface. Scans after argon etching should represent samples free of alterations during sample handling. The spectrum for the outer surface (blue line) was similar to that of pitchblende (U_3O_8) with a characteristic peak at 381.1eV (Wersin et al., 1994; Allen et al., 1974). The red line for the etched sample was consistent with uraninite (UO_2) with a characteristic peak at 380.6eV (Chadwick, 1973; Allen et al., 1974; Wersin et al., 1994).

In the XPS spectra of S2*p* (Fig. A4(b)), the two blue lines represented the outer surface of FeS loaded with U and pure FeS, respectively, and two red lines the spectra after slight etching of 75 Å off the surface. No significant difference existed with and without the surface etching for the sample loaded with U and the sample of pure FeS. However, after reaction with U, the S 2*p* spectra showed split peaks centered at 161.7eV and 162.6 eV, indicating the presence of polysulfide (Cantrell et al., 2003; Ko and Chu, 2005).

The XPS spectra of Fe2*p* for FeS loaded with U and pure FeS were shown in Fig. A4(c), with and without surface etching. The result suggested that Fe(III) was not produced in significant amount from the reaction with U(VI); otherwise, the spectra would have the characteristic peaks of Fe(III) oxide species at ~711eV and ~724eV (Wersin et al., 1994; Ko and Chu, 2005).

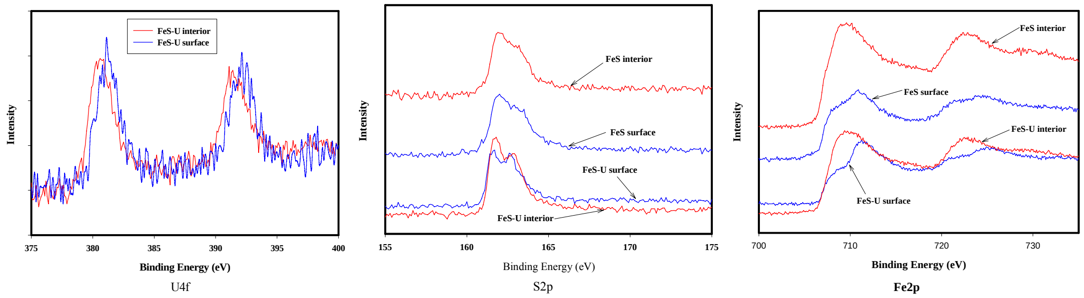

(a) (b) (c)

FIGURE A4. XPS spectra for FeS loaded with U prepared at pH 6.99. (a) U4*f* spectra; (b) S2*p* spectra; (c) Fe2*p* spectra.

Discussion

From the above observations, we propose the following 3-step mechanism to interpret the reductive precipitation of U(VI) by amorphous FeS.

Step 1

$$\equiv FeS^- + H^+ \leftrightarrow \equiv FeSH \qquad (1)$$

Step 2

$$\equiv FeSH \xrightarrow{UO_2^{2+}} \equiv UO_2 - SH + Fe^{2+} \qquad (2)$$

Step 3

$$\equiv UO_2 - SH + H_2O \rightarrow \equiv U_3O_8 / UO_2 + \equiv polysulfide + H^+ \qquad (3)$$

where ≡ designates the species associated with FeS. The protonation/deprotonation of the FeS surfaces (step 1) is assumed to be fast. Upon mixing of FeS and U(VI), uptake of U(VI) occurs through an ion exchange process forming ≡U(VI)-SH species, with concurrent releases of Fe(II) into the solution (Step 2). Intramolecular electron transfer within ≡U(VI)-SH yields U_3O_8/UO_2 and polysulfide as products (Step 3).

Uptake of U(VI) by FeS. The results in Fig. A1 indicate that the uptake of U(VI) from the aqueous phase by FeS is accompanied by the release of Fe(II). The experiments at pH 6.90 shown in Fig. A2 further verify a linear correlation between the amount of U(VI) uptake and Fe(II) release: $[U]_{uptake} = 0.85\ x[Fe(II)]_{released}$ ($R^2 = 0.995$). We, therefore, believe that the uptake of U(VI) is through an ion exchange mechanism: Fe(II) is replaced by U(VI), leading to the observed U(VI) phase transfer (Step 2). A schematic cartoon illustrating this ion exchange process is shown in Fig. A5. An alternative explanation for the disappearance of U(VI) from the aqueous phase could also be proposed: U(VI) is precipitated as minerals such as schoepite. Under the circumneutral conditions, this is, however, not supported by our preliminary experiments that showed no U(VI) precipitation in the FeS-free solution with ~168μM U(VI) at pH6.90, an observation consistent with other reported studies (Sani et al., 2004; Fredrickson et al., 2004).

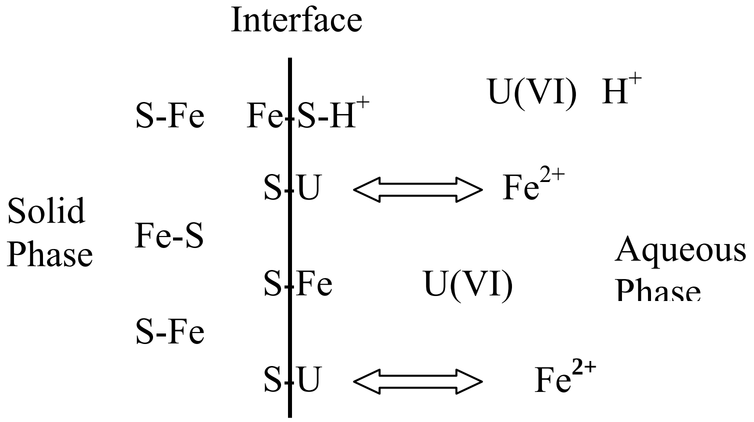

FIGURE A5. A schematic diagram of the pathway for the sorption of U(VI) by FeS.

In comparison with U(VI) sorption at pHs 5.99 and 6.90 where the ion exchange mechanism is operative, interpretation of U(VI) uptake at higher pH is confounded by that fact that the release of Fe(II) is much smaller than the stoichiometric amount of U(VI) uptake (Fig. A1). A possible explanation is that the released Fe(II) hydrolyzes to form $Fe(OH)_2$ precipitates, decreasing the soluble Fe(II) that could be detected. We have tested this hypothesis by calculating the equilibrium distribution of Fe(II) as a function of pH at a total Fe(II) concentration of 168.0 μM, using a common speciation program, MINEQL+ (version 4.07). As shown in Fig. A6, soluble ferrous iron ($[Fe(II)]_{aq}$) stays constant at 168.0 μM from pH 5.0 to 7.6, then decreases by 3 orders of magnitude when pH is increased from 7.7 to 8.7. The calculated $[Fe(II)]_{aq}$ are 30 μM, 0.7 μM, and 4.8×10^{-3} μM at pH 8.0, 8.8 and 10.2, respectively. In comparison, the observed amounts of sorption are 56 μM, 18.9 μM, and 7.9 μM, respectively. Given the detection limit of Fe(II) (0.2 μM) and the variation of background $[Fe(II)]_{aq}$ (± 5 μM), the observed values of $[Fe(II)]_{aq}$ agree qualitatively with the calculation, suggesting that the ion exchange process still occurs under the alkaline condition. This explanation is not conclusive, however, because we can not rule out the possibility that partial precipitation of U(VI) occurs in the alkaline solution, without exchanging Fe(II).

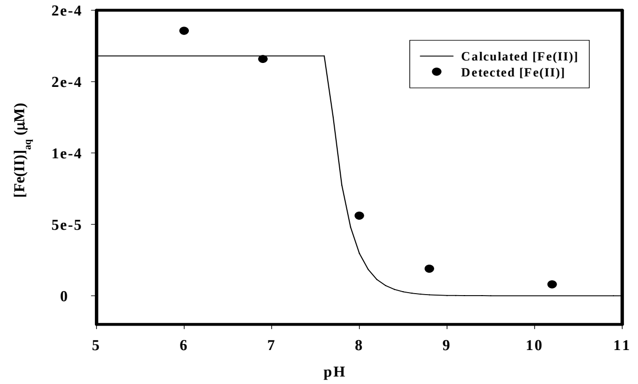

FIGURE A6. Variations of $[Fe(II)]_{aq}$ with pH. The curve was calculated with MINEQL+ (version 4.07) ($[Fe(II)]_0$=168.3 μM). The experimentally detected $[Fe(II)]_{aq}$ were incorporated in the figure as the doted points.

It appears that the involvement of U(VI) in an ion exchange process is not unique that only applies for amorphous FeS. Our preliminary experiments show that at pH 6.20, U(VI) uptake by lead sulfide (PbS, synthesized by mixing equal molar concentrations of $Pb(NO_3)_2$ and Na_2S solutions) is also accompanied by the release of lead(II) and complete reduction within 24 hr: 145.0 μM of Pb(II) being released with the uptake of 168.0μM U(VI). Our observation agrees with the result by Wersin et al. (1994), who found that the sorption of U(VI) by galena was accompanied by the release of lead and partial reduction of U(VI). Wersin et al. (1994) also found that the $[Pb(II)]_{aq}$ was proportional to the adsorbed [U(VI)], although $[Pb(II)]_{aq}$ is much less than the sorbed amount of [U(VI)].

Reduction of $U(VI)_{(s)}$. In the system examined here, potential reductants include $Fe(II)_{(aq)}$, $HS^-_{(aq)}$, $Fe(II)_{(s)}$, and $HS^-_{(s)}$. When we assume a first order kinetics with respect to each species, a generic expression for the total rate of U(VI) reduction can be formulated as:

$$-\frac{d[U(VI)]_T}{dt} = k_1[Fe(II)]_{aq}[U(VI)]_{aq} + k_2[HS^-]_{aq}[U(VI)]_{aq}$$
$$+ k_3[Fe(II)]_s[U(VI)]_{aq} + k_4[HS^-]_s[U(VI)]_{aq}$$
$$+ k_5[Fe(II)]_s[U(VI)]_s + k_6[HS^-]_s[U(VI)]_s \qquad (4)$$

The reduction of $U(VI)_{(aq)}$ by $Fe(II)_{(aq)}$ is thermodynamically unfavorable unless under strong acidic conditions (Gu et al., 1998). Furthermore, Liger et al. (1999) experimentally demonstrated that $Fe(II)_{(aq)}$ could not reduce $U(VI)_{(aq)}$ at pH 7.5. As a result, the first term on the right-hand side (RHS) in Equation 4 can be ruled out.

Aqueous HS^- can reduce U(VI) under certain conditions with a typical half-life of hours (Beyenal et al., 2004; Hua et al., 2006). However, the second term is unlikely to be a major mechanism here. As shown in Fig. A1, over 90% of U(VI)(aq) has been removed by FeS within 15 min (except for pH 10.17, in which case slightly longer time was involved), leading to virtually complete transformation of U(VI)$_{(aq)}$ to U(VI)$_{(s)}$. Consequently, the second term as well as the fourth term on the RHS of Eq. 4 can be omitted too.

If the sorbed Fe(II) had been the major species for the reduction of U(VI) in our system, [Fe(II)]$_{aq}$ would have been observed to be decreasing as the [U(VI)]$_{ex}$ decreased. The results shown in Fig. A1(b), however, do not support this mechanism. The XPS results shown in Fig.A4(c) further ruled out the solid Fe(II) species as the major reductant. As a result, the third and fifth terms on RHS can be eliminated. In an experiment to evaluate the influence of sediment on uranium sorption, Liu et al. (2005) also did not observe any reduction of aqueous or adsorbed U(VI) by sorbed Fe(II).

We believe U(VI)$_{(s)}$ is more likely reduced by HS$^-_{(s)}$ and Equation (4) is therefore reduced to Equation (5). The sorption of U(VI) by FeS indicates an ion exchange mechanism (at least at acidic pHs), suggesting the formation of [≡*U(VI)-SH*] complexes, where U(VI) should take the positions of Fe(II) in FeS. Indeed, the results in Fig. A4(a) and (b) confirmed that U(VI)$_{(s)}$ was reduced to U_3O_8/UO_2 with the oxidation of HS$^-_{(s)}$ to polysulfide. In addition, the reduction of U(VI) by Galena (Wersin et al., 1994) and PbS (our prelimianry data) also support this conclusion, since there is no evidence showing Pb^{2+} can reduce U(VI).

$$-\frac{d[U(VI)(s)]}{dt} = k[HS^-{}_{(s)}][U(VI)_{(s)}] \qquad (5)$$

To quantitatively evaluate the reduction of U(VI)$_{(s)}$, the change of [U(VI)]$_s$ as a function time must be obtained. Although [U(VI)]$_s$ can not be directly measured, [U(VI)]$_{ex}$ can and the two variables are equivalent as long as U(VI) uptake is completed. The time needed for the completion of U(VI) uptake can be determined in Fig.A3(a), which showed that over 90% of U(VI)(aq) has been transferred to FeS after 15min for pH 5.99 and 6.90, 1 hour for pH 7.99 and 10.17, and 2 hours for pH 8.82. As a result, we think [U(VI)]$_s$=[U(VI)]$_{ex}$ from the corresponding time points and a plot of ln([U(VI)]$_s$/[U(VI)]$_{s0}$) as a function of time was shown in Fig.A3(b), where [U(VI)]$_{s0}$ is the concentration of U(VI) associated with FeS at the time point when U(VI) uptake is considered to be completed. The linear relationship in Fig. A3(b) suggests that the reduction of U(VI)$_{(s)}$ follows a pseudo-first-order law with respect to [U(VI)]$_s$.

$$-\frac{d[U(VI)_{(s)}]}{dt} = k_{obs}[U(VI)_{(s)}] \qquad (6)$$

As shown in Fig. A3(b), k_{obs} values (slopes of the straight lines in Fig. A3(b)) strongly depend on pH, suggesting that k_{obs} is proportional to [≡*SH*] instead of *TOTS* as shown in Equation (4). Using Equation (7) to represent the relationship between [≡*SH*] and *TOTS*, the relationship between k_{obs} in Equation (6) and k in Equation (5) can be expressed in Equation (8).

$$[\equiv SH] = \frac{[H^+]}{[H^+]+K_a} \times TOTS \qquad (7)$$

$$\frac{1}{k_{obs}} = \frac{K_a}{k}\frac{1}{[H^+]} + \frac{1}{k} \qquad (8)$$

k is the real reduction rate constant, and K_a is the equilibrium constant for Equation (1) (Step 1). Indeed, plotting $1/k_{obs}$ with $1/[H^+]$ yielded a straight line with a slope of 1.0e-8 (R^2=0.98) and K_a = 1.2e-9 (pK_a = 8.9). Wolthers et al. (2005) recently reported that zero point charge of disordered machinawite is approximately 7.5, which is comparable with our pK_a.

In short, this study has demonstrated that the reductive precipitation of U(VI) by synthesized, amorphous iron sulfide follows an ion exchange and reduction processes. The uptake of U(VI) is rapid and insensitive to pH, while reduction strongly depends on pH. Cantrell et al. (2003) found iron oxides at the contaminated sits could be reduced by injected hydrogen sulfide gas. Therefore, a permeable reactive barrier (PRB) of FeS could be created by the injection of hydrogen sulfide gas to the contaminated sites with high iron contents. According to this research, PRB of FeS should have a high potential to prevent the subsurface migration of U(VI). Since FeS could also be produced in the contaminated sites tested for biostimulation with ethanol (Wu et al., 2006) or acetate (Anderson et al., 2003) for reductive U(VI) immobilization, the production of FeS coupled with sulfate reduction likely provides an abitic mechanism that could significantly contribute to U(VI) reduction. Much has been learned in this research regarding the fundamental mechanisms and reduction rate under the well-controlled laboratory conditions. Future work is needed to evaluate the impact of complex groundwater and soil constituents on the reduction kinetics.

Acknowledgments

This work was supported by the United States Department of Energy under the Environmental Remediation Science Program (ERSP) (Grant No. DE-FG02-03ER63616).

Literature Cited

[1] Langmuir, D. Uranium solution-mineral equilibria at low temperatures with applications to sedimentary ore deposits. *Geochim. Cosochim. Acta*, **1978**, *42*, 547-569.

[2] Hsi, C. D.; Langmuir, D. Adsorption of uranyl onto ferric oxyhydroxides: Application of the surface complexation site-binding model. *Geochim. Cosmochim. Acta* **1985**, *49*, 1931-1941.

[3] Ho, C. H.; Doern, D. C. The sorption of uranyl species on the hematite sol. *Canadian, J. Chem.* **1985**, *63*, 1100-1105.

[4] Ho, C. J.; Miller, N. H. Adsorption of uranyl species from bicarbonate solution onto hematite particles. *J. Colloid Interfacial Science* **1986**, *110*, 165-171.

[5] Payne, T. E.; Waite, T. D. Surface complexation modeling of uranium sorption data obtained by isotope exchange techniques. *Radiochim. Acta* **1991**, *52/52*, 487-494.

[6] Wersin, P.; Hochella Jr., M. F.; Persson, P.; Redden, G.; Leckie, J. O.; Harris, D. W. Interaction between aqueous uranium(VI) and sulfide minerals: spectroscopic evidence for sorption and reduction. *Geochim. Cosmochim. Acta* **1994**, *58*, 2829-2843.

[7] Moyes, L. N.; Parkman, R. H.; Charnock, J. M.; Vaughan, D. J.; Livens, F. R.; Hughes, C. R.; Braithwaite, A. Uranium uptake from aqueous solution by interaction with goethite, lepidocrocite, muscovite, and mackinawite: an X-ray absorption spectroscopy study. *Environ. Sci. Technol.* **2000**, *34*, 1062-1068.

[8] Giammer, D. E.; Hering, J. G. Time scales for sorption-desorption and surface precipitation of uranyl on goethite. *Environ. Sci. Technol.*, **2001**, *35*, 3332-3337.

[9] Liger, E.; Charlet, L.; Van Cappellen, P. Surface catalysis of uranium(VI) reduction by iron(II). *Geochim. Cosmochim. Acta* **1999**, *63*, 2939-2955.

[10] Waite, T. D.; Davis, J. A.; Payne, T. E.; Waychunas, G. A.; Xu, N. Uranium(VI) adsorption to ferrihydrite: application of a surface complexation model. *Geochim. Cosmochim. Acta* **1994**, *58*, 5465-5478.

[11] Villalobos, M.; Trotz, M. A.; Leckie, J. O. Surface complexation modeling of carbonate effects on the adsorption of Cr(VI), Pb(II), and U(VI) on goethite. *Environ. Sci. Technol.* **2001**, *35*, 3849-3856.

[12] Cheng, T.; Barnett, M. O.; Roden, E. E.; Zhuang, J. Effects of phosphate on uranium (VI) adsorption to goethite-coated sand. *Environ. Sci. Technol.* **2004**, *38*, 6059-6065.

[13] Lenhart, J.J.; Honeyman, B.D. Uranium (VI) sorption to hematite in the presence of humic acid. *Geochim. Cosochim. Acta* **1999**, *63*, 2891-2901.

[14] Posey-Dowty, J.; Axtmann, E.; Crerar, D.; Borcsik, M.; Ronk, A.; Woods, W. Releasing rate of uraninite and uranium roll-front ores. *Economic Geology and the Bulletin of the Society of Economic Geologists* 1987, **82**(1), 184-194.

[15] O'Loughlin, E. J.; Kelly, S. D.; Cook, R. E.; Csencsits, R.; Kemner, K. M. Reduction of uranium (VI) by mixed iron (II)/ iron (III) hydroxide (green rust): formation of UO_2 nanoparticles. *Environ. Sci. Technol.* **2003**, *37*, 721-727.

[16] Missana, T.; Maffiotte, C.; Miguel, G. Surface reactions kinetics between nanocrystalline magnetite and uranyl. *Colloid and Interface Science*. **2003**, *261*,154-160.

[17] Nevin, K. P.; Lovley, D. R. Potential for nonenzymatic reduction of Fe(III) by electron shuttling in subsurface sediments. *Environ. Sci. Technol.* **2000**, *34*, 2472-2478.

[18] Istok, J. D.; Senko, J. M.; Krumholz, L. R.; Watson, D.; Bogle, M. A.; Peacock, A.; Change, Y.-J.; White, D. C. In situ bioreduction of technetium and uranium in a nitrate-contaminated aquifer. *Environ. Sci. Technol.* **2004**, *38*, 468-475.

[19] Kochenov, A.V.; Korolev, K.G.; Dubinchuk, V. T.; Medvedev, Y. L. Experimental data on the conditions of precipitation of uranium from aqueous solutions. *Geochemistry International* **1978**, *14*, 82-87.

[20] Duff, M. C.; Amrhein, C.; Bertsch, P. M.; Hunter, D. B. The Chemistry of uranium in evaporation pond sediment in the San Joaquin Valley, California, USA, using X-ray fluorescence and XANES techniques. *Geochim. Cosochim. Acta* **1997**, *61*, 73-81.

[21] Beyenal, H.; Sani, R. K.; Peyton, B. M.; Dohnalkova, A. C.; Amonette, J. E.; Lewandowski, Z. Uranium immobilization by sulfate-reducing biofilms. *Environ. Sci. Technol.* **2004**, *38*, 2067-2074.

[22] Hua, B. and Deng, B. Kinetics of uranium(VI) reduction by hydrogen sulfide in anoxic aqueous systems. *Environ. Sci. Technol.* **2006,** *40*, 4666-4671.

[23] Patterson, R. R.; Fendorf, S.; Fendorf, M. Reduction of hexavalent chromium by amorphous iron sulfide. *Environ. Sci. Technol.* **1997**, *31*, 2039-2044.

[24] APHA. *Standard methods for the examination of water and wastewater;* 17th ed.; American public Health Association: Washington, DC, 1989.

[25] JCPDS. *Power diffraction file alphabetical index, inorganic phases.* JCPDS, International Center for Diffraction Data, 1987.

[26] Teixeira, L.S.G.; Costa, A.C.S.; Ferreira, S. L. C; Freitas, M. L.; Carvalho, M. S. Spectrophotometric determination of uranium using 2-(2-thiazolylazo)-p-cresol(TAC) in the presence of surfactants. *J. Braz. Chem. Soc.* **1999**, *10*(6), 519-522.

[27] Buck, E. C.; Brown, N. R.; Dietz, N. L. Contaminant uranium phases and leaching at the Fernald site in Ohio. *Environ. Sci. Technol.* **1996,** *30*, 81-88.

[28] Allen, G.C.; Crofts, J.A.; Curtis, M.T.; Tucker, P.M.; Chadwick, D.; Hampson, P.J. X-ray photoelectron spectroscopy of some uranium oxide phases. *J. Chem. Soc. Dalton Trans.,* **1974**, 1296-1301.

[29] Chadwick, D. Uranium 4f binding energies studies by X-ray photoelectron spectroscopy. *Chem. Phys. Lett.* **1973**, *21*, 291-294.

[30] Cantrell, K.J.; Yabusaki,S.B.; Engelhard, M.H.; Mitroshkov, A.V.; Thornton, E.C. Oxidation of H_2S by iron oxides in unsaturated conditions. *Environ. Sci. Technol*., **2003**, *37*, 2192-2199.

[31] Ko, T. H.; Chu, H. Spectroscopic study on sorption of soil hydrogen by means of red soil. *Spectrochimica Acta Part A: Molecular and Biomolecular Spectroscopy* **2005**, *61*, 2253-2259.

[32] Sani, R. K; Peyton, B. M.; Amonette, J. E.; Geesey, G. G. Reduction of uranium(VI) under sulfate-reducing conditions in the presence of Fe(III)-(hydr)oxides. *Geochim. Cosochim. Acta* **2004**, *68*, 2639-2648.

[33] Fredrickson, J. K.; Zachara, J. M.; Kennedy, D. W.; Dong, H.; Onstott, T. C.; Hinman, N. W.; Li, S. Biogenic iron mineralization accompanying the dissimilatory reduction of hydrous ferric oxide by a groundwater bacterium. *Geochim. Cosmochim. Acta* **1998**, *62,* 3239– 3257.

[34] Gu, B.; Liang, L.; Dickey, M.J.; Yin, X.; Dai, S. Reductive precipitation of uranium(VI) by zero-valent iron. *Environ. Sci. Technol*., **1998**, *32*, 3366-3373.

[35] Liu, C.; Zachara, J. ; Zhong, L.; Kukkapdupa, R.; Szecsody, J. E.; Kennedy, D. W. Influence of sediment bioreduction and reoxidation on uranium sorption. *Environ. Sci. Technol.* **2005**, *39*, 4125-4133.

[36] Wolthers, M.; Charlet, L.; van Der Linde, P. R.; Rickard, D.; van Der Weijden, C. H. Surface chemistry of disordered mackinawite (FeS). *Geochimica et Cosmochimica Acta* **2005**, *69*(14), 3469-3481.

[37] Wu W. M., Carley J., Fienen M., Mehlhorn T., Lowe K., Nyman J., Luo J., Gentile M. E., Rajan R., Wagner D., Hickey R. F., Gu B., Watson D., Cirpka O. A., Kitanidis P. K., Jardine P. M., and Criddle C. S. Pilot-scale in situ bioremediation of uranium in a highly contaminated aquifer. 1. Conditioning of a treatment zone. *Environ. Sci. Technol.* **2006**, 40, 3978-3985.

[38] Anderson R. T., Vrionis H. A., Ortiz-Bernad I., Resch C. T., Long P. E., Dayvault R., Karp K., Marutzky S., Metzler D. R., Peacock A., White D. C., Lowe M., and Lovley D. R. Stimulating the in situ activity of Geobacter species to remove uranium from the groundwater of a uranium-contaminated aquifer. *Applied and Environmental Microbiology, **2003**,* 69(10), 5884-5891.